CFD Letters

The Effect of Blade Height and Inlet Height in a Straight-Blade Undershot Waterwheel Turbine by Computational Method

Open Access

Warjito[1], Dendy Adanta[1], Budiarso[1], Sanjaya BS Nasution[1], Muhamad Agil Fadhel Kurnianto[1,*]

[1] Department of Mechanical Engineering, Faculty of Engineering, University of Indonesia, Depok 16424, West Java, Indonesia

ARTICLE INFO	ABSTRACT
	The potential of renewable energy in Indonesia is very high, especially for hydropower: 75 GW can be obtained from a large scale, and 19 GW from a mini, micro and pico scale. However, in 2018, there were 5 million people in Indonesia lacking access to electricity. A pico hydro-type undershot waterwheel is one suitable solution to this problem. The undershot waterwheel was chosen for this study because its design, operation, maintenance and installation is believed to be simpler than other types of turbines. Although this turbine technology is quite dated compared to other types, there has been no particular discussion about the effect of blade height (h) and inlet height (L) on the power produced. This study therefore investigates the influence of h and L on power production by using CFD tools. This study uses six degrees of freedom (6-DoF) for the transient approach, and the standard $k - \varepsilon$ turbulent model to predict turbulent flow. Based on the results, the h/L ratio has an influence on the performance of undershot waterwheel. An h/L ratio of 1 produces greater power than ratios of 0.5, 0.75 or 1.5. The resulting efficiency with an h/L ratio of 1 is 31.52 %, while with 0.5 it is 22.75 %, with 0.75 it is 29.44 % and with 1.5 it is 26.55 %. Thus, an h/L ratio of 1 is recommended for designing undershot waterwheel turbines.

1. Introduction

The potential of renewable energy in Indonesia is very high, especially for hydropower: 75 GW can be obtained from a large scale , and 19 GW from a mini, micro and pico scale [1] . Although these numbers seem convincing, there are still regions of Indonesia that don't have access to electricity, particularly in remote areas. The latest report states that there are around 5 million Indonesians who do not have access to electricity, especially in remote areas due to the difficulty of accessing the region. The fact is that the economy and improvement of people's living standards are both very dependent on electricity usage. To overcome electricity problem, pico hydro turbines are considered particularly suitable to apply, especially for rural communities [2].

A pico hydro turbine is a hydropower plant with an ability to produce electricity below 5 kW [3]. Pico hydro turbines can also be more easily designed, developed and operated than solar PV systems or wind turbines. Furthermore, pico hydro technology appears to be the most well-known technology

---

* *Corresponding author.*
E-mail address: agil.fadhel@gmail.com (Muhamad Agil Fadhel Kurnianto)

among most people in Indonesia [4]. One type of pico hydro technology that is familiar in Indonesia is the undershot waterwheel. The undershot waterwheel was chosen because its design, operation, maintenance and installation is believed to be simpler than other types of turbines [4]. The only disadvantage of this turbine technology is its low efficiency [4].

To improve undershot waterwheel turbine performance, there are three types of methods that are often used: analytical, computational and experimental. Computational methods, especially computational fluid dynamics (CFD) tools, are currently widely used to solve fluid dynamics problems. This is because CFD tools can analyse a system to reduce the cost of the experiment as well as the time to conduct it. They can also help shorten the design stage of the engineering process [5]. 6-DoF is used as an exact determination for simulation of pico hydro turbine [6-7]. Pujol *et al.,* [8] characterized undershot waterwheels using laboratory scale test data. Characterization results were used as a basis for improving turbine performance using CFD tools. Nishi *et al.,* [9] compared the performance of straight and curved blade shapes in undershot waterwheel turbines using CFD tools. Based on the results, the straight blade shape was found to be more effisien than the curved shape. Yah *et al.,* [10] investigation on effect immersed blade depth on the undershot waterwheel or the straight blades turbine which consists of 6 blades. The result is optimum immersed depth which is 40 mm before decreasing [10]. Warjito *et al.,* [4] proposed a number of blade equations for undershot waterwheel turbines. The proposed equations were tested using CFD tools, and were concluded to be verified and usable. Based on this literature, blade shape has an important role in the power generation of undershot waterwheel turbines. However, the influence of ratio of the outer diameter (D_o) and the inner diameter (D_i), or blade height (h), on the power to be generated has not yet been examined in a comprehensive study. Denny's [11] undershot water turbine has a ratio value (v/U) for the inlet velocity (v) with a rotational velocity of wheel (U) of 0.33. In his research [11], it was assumed that there was no loss of energy (due to, for example, splashing water) or wheel spokes, which influence the results of analytical calculations. Rinaldi *et al.,* [12] conducted an experimental study of the physical model of a waterwheel as a generator. The researchers formulated the available power from high water fall and flat-water flow.

Based on previous studies, the blade height (h) is one of the parameters for the power to be produced, because the turbine rotation velocity of the wheel (U) is a function of the moment of inertia (I) of the wheel, while the I is influenced by the h. Although this turbine technology is quite old compared to other types, researchers have paid no attention to the effect of h and inlet height (L) on the power to be produced. This study will therefore investigate the influence of h and L on power to be produced by using CFD tools with the six degrees of freedom (6-DoF) feature. CFD tools with the 6-DoF feature were used because the turbine rotation is a computational result, which is similar to actual conditions [13].

2. Methodology
2.1 Geometry

The specific wheel geometry design in this study is based on Warjito's study [4]. In this simulation, the number of blades is constant, with a variable value for the ratio of blade height to head inlet (h/L) set to 0.5, 0.75, 1 and 1.5. The design of the turbine geometry shown in Table 1. Figure 1 shows the models of the undershot water wheel.

Table 1
Design of the turbine geometry

Design Parameter	Dimension
Blade Height, h	0.164 m
Inner Diameter, D_i	0.820 m
Outer Diameter, D_o	0.984 m
Blade Width, W	0.240 m
Number of blades, z	8 blades
Blade Angle, θ	45^0
Blade Thickness, t	0.002 m

(a) Three-dimensional model of wheel   (b) Two-dimensional model of wheel
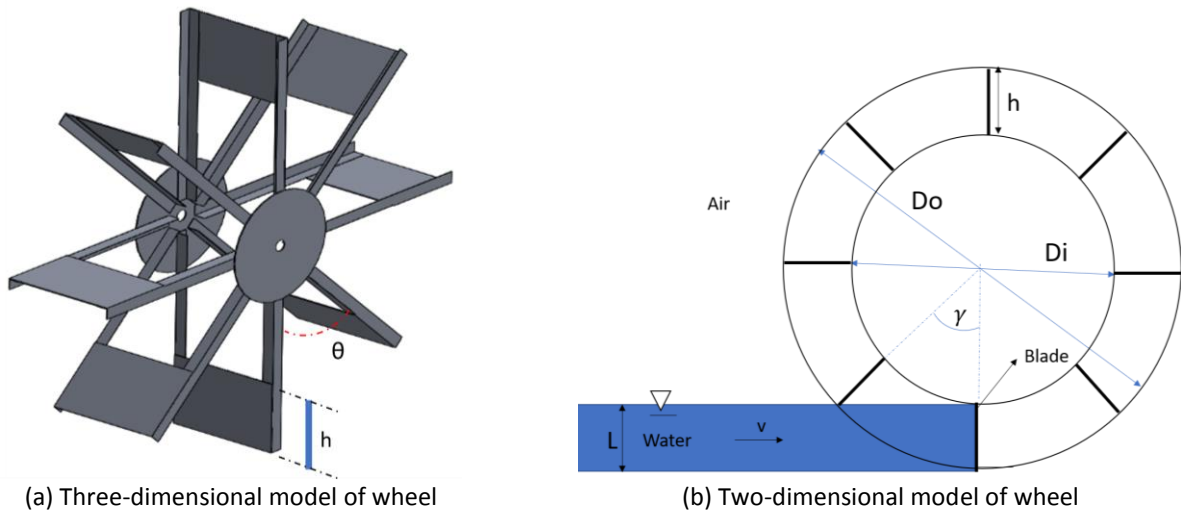
Fig. 1. The Undershot water wheel design

2.2 Computational Method

The simulation of the undershot waterwheel was conducted using ANSYS Fluent 18.1 in a two-dimensional (2D) flow analysis. Figure 2 shows the 2D domain mesh visualization.
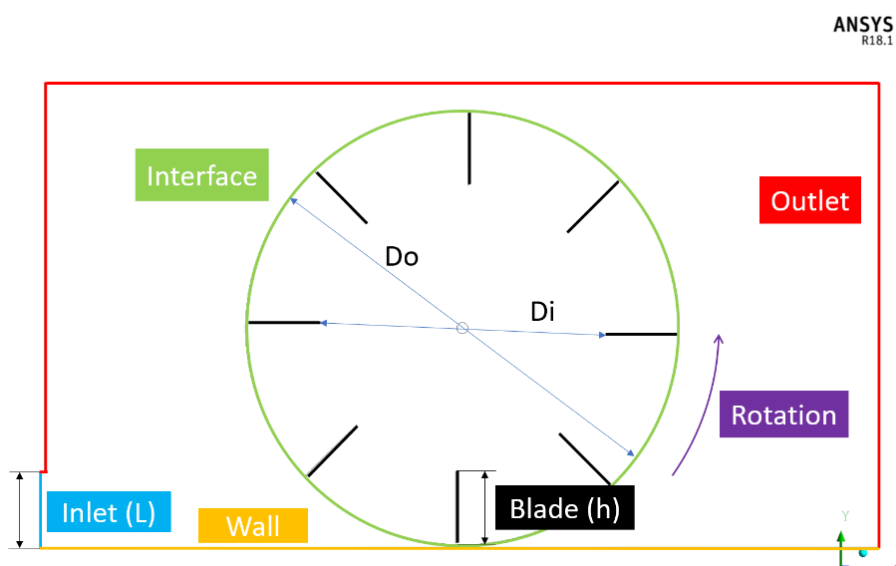
Fig. 2. 2D Domain mesh visualization – 50969 elements

Boundary conditions: The simulation is for the straight-blade waterwheel, which consists of 8 blades, and the velocity inlet (v) of the river is considered to be 1 m/s. The simulations were run using standard Volume of Fluid (VoF) multiphase modelling with constant interfacial surface tension, implicit volume fraction parameters and implicit body force. The VoF setting was enabled because there were two fluid phases, water and air, with a constant surface tension value of 0.0728 N/m between these fluids [7].

Dynamic mesh settings were also activated to enable the six degrees of freedom (6-DoF) feature, where 6-Dof used the object's forces and moments in order to calculate the translational and angular motion of its centre of gravity. In this case, 6-DoF was used to investigate the phenomenon of fluid dynamics, with the movement of domain blades that occur from interactions with fluids. The equation for the translational motion of the centre of gravity is solved for the inertial coordinate system [14]:

$$\overrightarrow{V_G} = \frac{1}{m} \sum_{k=0}^{n} \overrightarrow{f_G}$$ (1)

where V_G is the translational motion, $\overrightarrow{f_G}$ is the force of gravity, and m is the mass. The angular motion of the object (ω_B) is further computed using body coordinates (Eq. (2)) [14]:

$$\overrightarrow{\omega_B} = L^{-1}(\sum \overrightarrow{M_B} - \overrightarrow{\omega_B} \, x \, \overrightarrow{L\omega})$$ (2)

Where L is inertia, M_B is moment of inertia of the body, and ω_B is the rigid body angular velocity.

If the 6-DoF property option is activated, the value for the moment of inertia is entered into the undershot water wheel simulation. The moment of inertia was obtained from the computer-aided design (CAD) software. Preload values were also activated for the 6-DoF simulations and were given as 3 N.m.

The standard $k - \varepsilon$ turbulence model is a model that is widely used in CFD to predict turbulent flow [15]. Standard $k - \varepsilon$ was chosen because of its accuracy and because many use it in the industry [14]. The standard $k - \varepsilon$ model was also chosen because based on its y⁺ value, the standard $k - \varepsilon$ model y⁺ has a range of average values of y⁺ in the range of 30-300 [16]. For this simulation case, the value of y⁺ blade obtained is 92.87. The governing equations of the standard $k - \varepsilon$ are available in Eq. (3) for k and Eq. (4) for ε, respectively [14]:

$$\frac{\partial}{\partial t}(\rho k) + \frac{\partial}{\partial t}(\rho k \, u_i) = \frac{\delta}{\delta x_i}\left[\left(\mu + \frac{u_t}{\sigma_k}\right)\frac{\sigma_k}{\sigma_{xj}}\right] + G_k + G_b - \rho\varepsilon - Y_M + S_k$$ (3)

and

$$\frac{\partial}{\partial t}(\rho\varepsilon) + \frac{\partial}{\partial t}(\rho k \, u_i) = \frac{\delta}{\delta x_j}\left[\left(\mu + \frac{u_t}{\sigma_\varepsilon}\right)\frac{\sigma_\varepsilon}{\sigma_{xj}}\right] + C_{1\varepsilon}\frac{\varepsilon}{k}(G_k + G_{3\varepsilon} + G_b) - C_{2\varepsilon}\rho\frac{\varepsilon^2}{k} + S_\varepsilon$$ (4)

2.3 Mesh and Timestep Independency Tests

The independence test serves to verify the number of mesh elements and timestep values that will be used later. Analysis of the independence test can be seen in previous studies [17-18]. In the mesh independence test, the variation of mesh was about 25196, 50969 and 101117 elements. The results of the independency mesh using the Richardson extrapolation method are shown in Table 2.

Table 2 shows the mesh independency test results. From the results of the GCI or Grid Convergen Independency, the figure of 50969 mesh elements was chosen because the margin of error was 0.55 %.
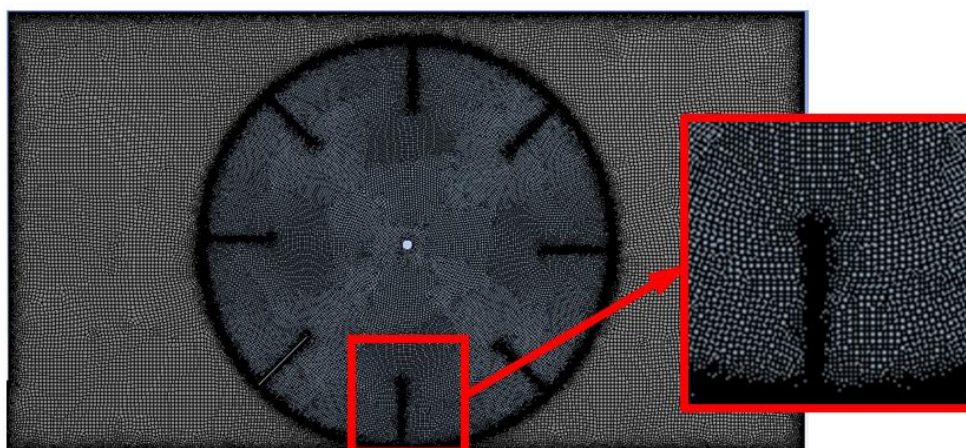
Table 2
Mesh independency test result

Number of Elements	Normalized Grid Spacing	Torque	GCI (%)
25196	2.00	32.11	3.62
50969	1.41	30.99	0.55
101117	1.00	30.82	0.10

This simulation was run with 5000 timesteps, with a timestep size of 0.001 s and 150 iterations for each simulation. The timestep size of 0.001 s was chosen because based on the Richardson extrapolation method, it has an error of 2.7 %. This is sufficient for the simulation because the error is below 3% [17]. Table 3 shows the results of the Timestep Independency Test. Figure 3 shows the mesh visualization with 50969 elements.

Table 3
Timestep independency test results

Timestep	Normalized Grid Spacing	Torque	GCI (%)
0.002	2.00	18.887	8.5
0.001	1.41	18.897	2.7
0.0005	1.00	18.954	0.35
0	0	18.955	

Fig. 3. 2D Domain mesh visualization – 50969 elements

3. Results
3.1 Results

Figure 4 shows the results of this simulation. Furthermore, Table 4 contains an interpretation of Figure 4. Figure 4(a) is a comparison graph of torque (τ) and timestep. Based on Figure 4(a), the torque (τ) obtained by the four blades fluctuates, and from timesteps 3000 to 5000 the torque obtained is steady. Figure 4(b) is a comparison graph of the rotational velocity of the wheel (U) and timestep. Based on Figure 4(b), a steady condition of the rotation velocity of wheel (U) occurs at timestep 2000. The torque(τ) and (U) data at steady conditions are in Table 4.

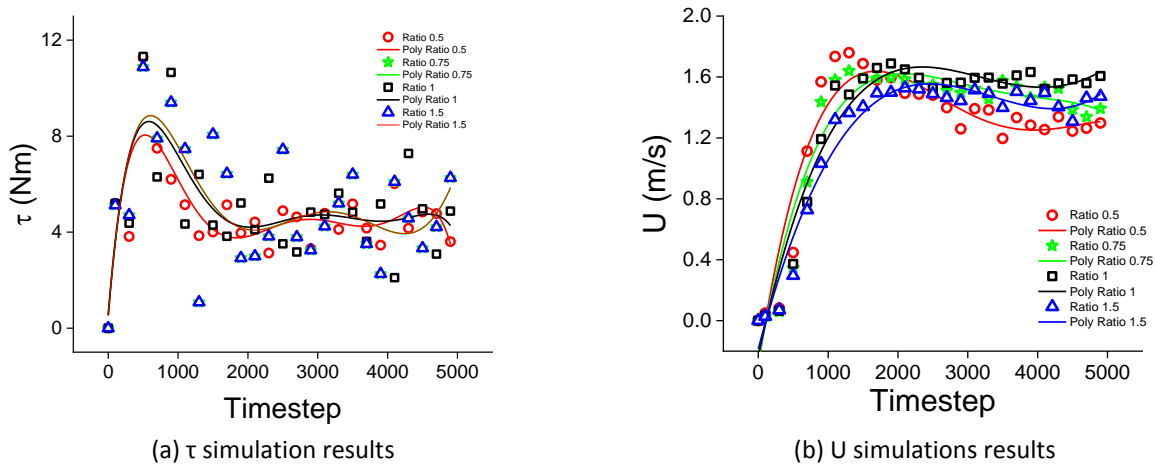(a) τ simulation results   (b) U simulations results

Fig. 4. The computational results

Table 4
Comparison of ration h/L with several parameters

Parameter	Ratio of h/L			
	0.5	0.75	1	1.5
Rotational wheel velocity stable, W -9.81	1.22 m/s	1.21 m/s	1.31 m/s	1.20 m/s
Torque stable, τ (N·m)	4.68	5.12	5.00	5.05
Power, P (Watt)	11.58	12.59	13.17	12.08
Efficiency, η (%)	22.75%	29.44%	31.52%	26.99%

3.2 Discussion

Based on Table 4, the undershot waterwheel with a ratio h/L of 1 has the blades with the highest average efficiency. Table 4 summarizes the computational results for variations of the h/L ratio. Based on Table 4, the best h/L ratio is 1, having an efficiency 31.52 % higher than the others. These results are roughly comparable to those of previous studies [11].The torque produced by the undershot turbine blade result from the hydrodynamic force between upstream and downstream. In Figure 5 (water pressure contour), there are black lines and red lines; black lines indicate upstream pressure (P_1) and red lines show downstream pressure (P_2). Based on Table 4, it appears that an h/L ratio of 0.5 produces torque under 0.75, 1 and 1.5. This is because the pressure gradient ($P_1 - P_2$ or ΔP) between the upstream and downstream of the active blade is small, and so the torque produced is also small (see Figure 5(a)). The ΔP at an h/L ratio of 0.5 is also low, due to an overflow of water that passes through the top of the active blade (see Figure 5(a)). Meanwhile, with an h/L ratio of 1 no water passes through the blade, so the hydrodynamic force is further absorbed into the power is produced by the turbine (see Figure 5(c)). With an h/L ratio of 1.5, the ΔP is greater than in the other cases. However, the low torque of the blade with the h/L ratio of 1.5 is suspected to result from the greater blade height. The greater blade height causes drag, because air pressure is increased (see Figure 6). Consequently, the rotation of the blade will decrease.

The results of this study verify the assumptions used by Warjito [4]. Warjito used the assumption that $h=L$ or $h/L = 1$. The results of this study are similar to Warjito's study [4]. Furthermore, these results also verify with Yah's study [10]. Yah [10] reports that a ratio of $h/D_o \sim 0.2$ produces maximum efficiency. In this case the maximum efficiency is obtained at the ratio of $h/D_o \sim 0.16$, which is equivalent to $h/L = 1$.
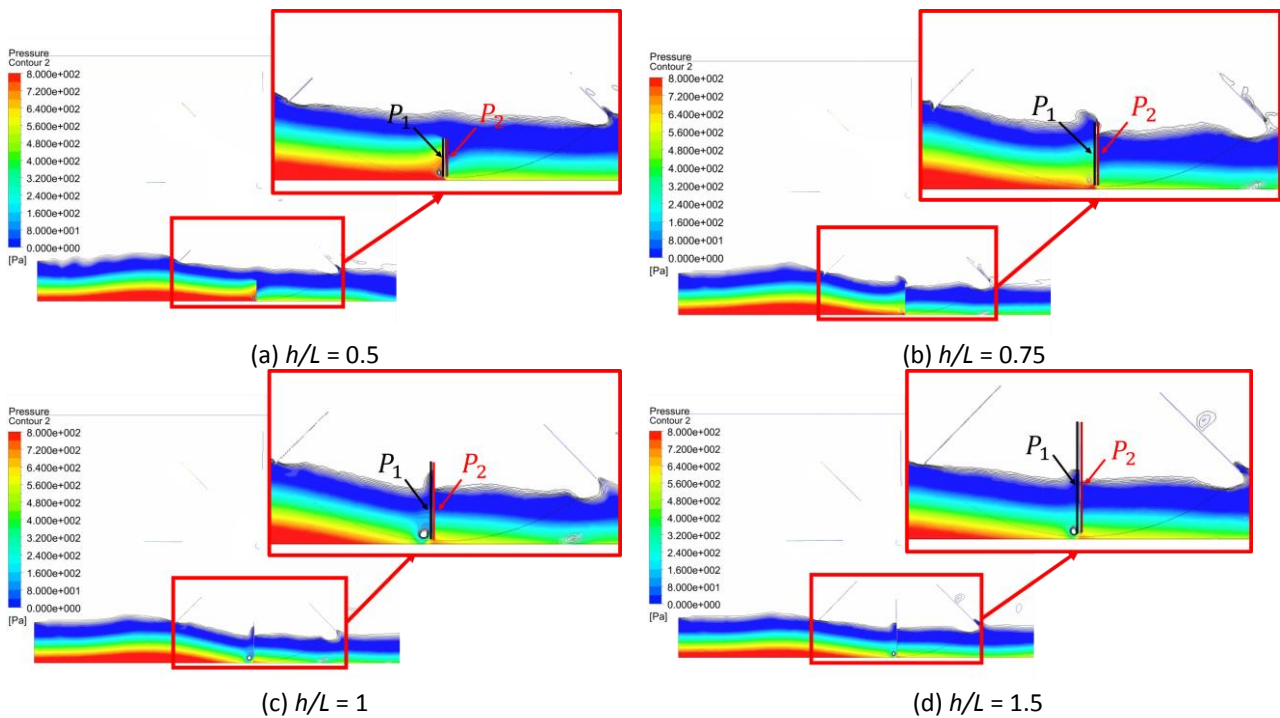
(a) *h/L* = 0.5

(b) *h/L* = 0.75

(c) *h/L* = 1

(d) *h/L* = 1.5

Fig. 5. Water pressure contour

(a) *h/L* = 0.5

(b) *h/L* = 0.75

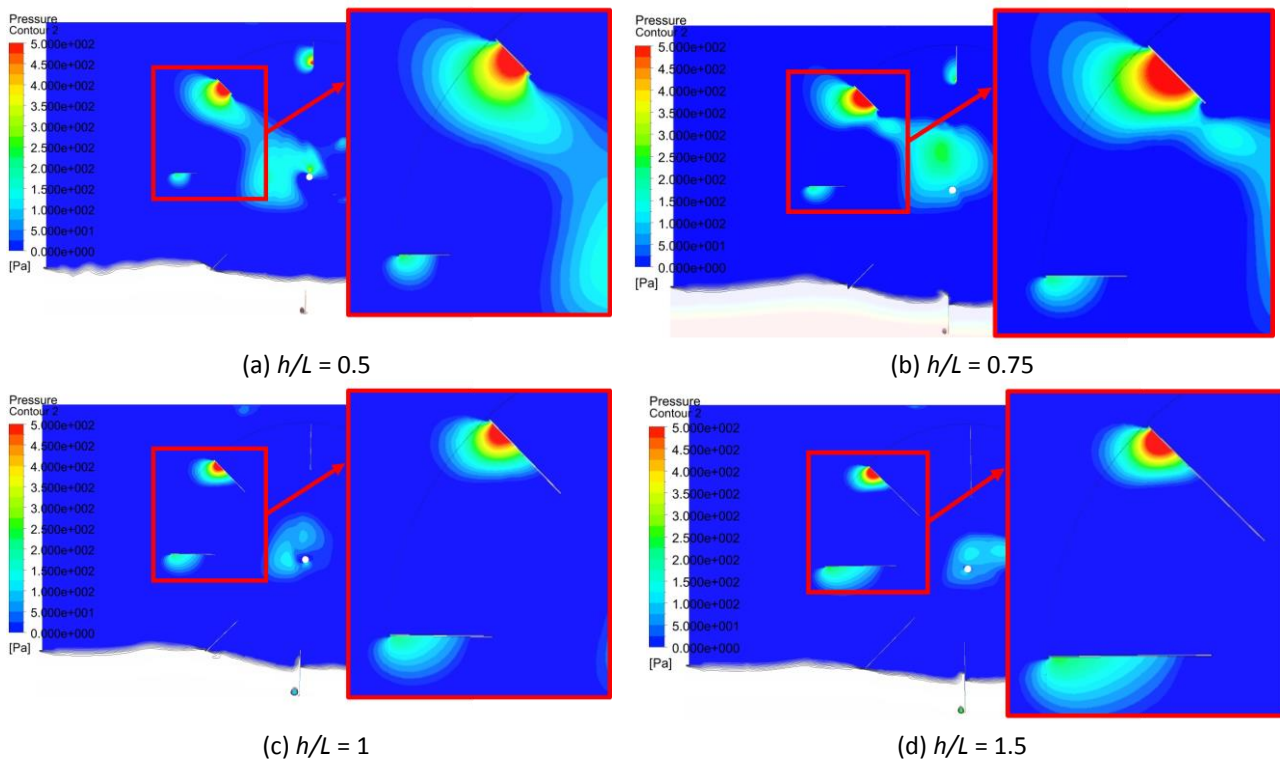(c) *h/L* = 1

(d) *h/L* = 1.5

Fig. 6. Air pressure contour

4. Conclusions

Based on these results, the h/L ratio has a significant influence on the performance of an undershot waterwheel. The h/L ratio of 1 produces power greater than 0.5, 0.75, and 1.5, and the resulting efficiency with an h/L ratio of 1 is 31.52 %, 0.5 is 22.75 %, 0.75 is 29.44 % and 1.5 is 26.55 %. Thus, an h/L ratio of 1 is recommended for designing undershot waterwheel turbines.

Acknowledgement

References

[1]   Humas EBTKE. "Menuju Rasio Elektrifikasi 99 Persen pada 2019." *Energi Baru Terbarukan dan Konservasi Energi (EBTKE)*, 2018.

[2]   Maher, P., N. P. A. Smith, and A. A. Williams. "Assessment of pico hydro as an option for off-grid electrification in Kenya." *Renewable Energy* 28, no. 9 (2003): 1357-1369.

[3]   G. Müller, "Renewable Energy -Muller WATER WHEELS AS A POWER SOURCE," pp. 1–9, 2007.

[4]   Adanta, Dendy, Satrio Adi Arifianto, and Sanjaya BS Nasution. "Effect of Blades Number on Undershot Waterwheel Performance with Variable Inlet Velocity." In *2018 4th International Conference on Science and Technology (ICST)*, pp. 1-6. IEEE, 2018.

[5]   Quaranta, Emanuele, and Roberto Revelli. "Hydraulic behavior and performance of breastshot water wheels for different numbers of blades." *Journal of Hydraulic Engineering* 143, no. 1 (2016): 04016072.

[6]   Adanta, Dendy, Warjito Budiarso, and Ahmad Indra Siswantara. "Assessment of turbulence modelling for numerical simulations into pico hydro turbine." *Journal of Advanced Research in Fluid Mechanics and Thermal Sciences* 46, no. 1 (2018): 21-31.

[7]   Siswantara, Ahmad Indra, Aji Putro Prakoso Budiarso, Gun Gun R. Gunadi, and Dendy Warjito. "Assessment of Turbulence Model for Cross-Flow Pico Hydro Turbine Numerical Simulation." *CFD Letters* 10, no. 2 (2018): 38-48.

[8]   Pujol, T., A. K. Vashisht, J. Ricart, D. Culubret, and J. Velayos. "Hydraulic efficiency of horizontal waterwheels: Laboratory data and CFD study for upgrading a western Himalayan watermill." *Renewable energy* 83 (2015): 576-586.

[9]   Nishi, Yasuyuki, Terumi Inagaki, Yanrong Li, Ryota Omiya, and Junichiro Fukutomi. "Study on an undershot cross-flow water turbine." *Journal of Thermal Science* 23, no. 3 (2014): 239-245.

[10]   Yah, Nor Fadilah, Mat Sahat Idris, and Ahmed Nurye Oumer. "Numerical investigation on effect of immersed blade depth on the performance of undershot water turbines." In *MATEC Web of Conferences*, vol. 74, p. 00035. EDP Sciences, 2016.

[11]   Denny, Mark. "The efficiency of overshot and undershot waterwheels." *European Journal of Physics* 25, no. 2 (2003): 193.

[12]   Akhiar Junaidi, R. Rinaldi, and Andy Hendri, "Model fisik kincir air sebagai pembangkit listrik," *Jom FTEKNIK*, 1, no. 2, (2014): 1–9.

[13]   Adanta, Dendy, and Aji P. Prakoso. "The effect of bucketnumber on breastshot waterwheel performance." In *IOP Conference Series: Earth and Environmental Science*, vol. 105, no. 1, p. 012031. IOP Publishing, 2018.

[14]   Fluent, A. N. S. Y. S. "ANSYS fluent theory guide 15.0." *ANSYS, Canonsburg, PA* (2013).

[15]   Launder, Brian Edward, G. Jr Reece, and W. Rodi. "Progress in the development of a Reynolds-stress turbulence closure." *Journal of fluid mechanics* 68, no. 3 (1975): 537-566.

[16]   Inc. ANSYS, "ANSYS FLUENT Theory Guide," *Release 18.2*, vol. 15317, no. November, pp. 373–464, 2013.

[17]   Phillips, Tyrone S., and Christopher J. Roy. "Richardson extrapolation-based discretization uncertainty estimation for computational fluid dynamics." *Journal of Fluids Engineering* 136, no. 12 (2014): 121401.

[18]   Adanta, D., Emanuele Quaranta, and T. M. I. Mahlia. "Investigation of the effect of gaps between the blades of open flume Pico hydro turbine runners." *Journal of Mechanical Engineering and Sciences* 13, no. 3 (2019): 5493-5512.